Polyelectrolyte Adsorption on a Charged Surface. Free Energy Calculation from Monte Carlo Simulations Using Jarzynski Equality

Claudio F. Narambuena,[†] Dante M. Beltramo,[‡] and Ezequiel P. M. Leiva*,[†]

Unidad de Matemática y Física, Facultad de Ciencias Químicas, Universidad Nacional de Córdoba, INFIQC, Córdoba, Argentina, Centro de Excelencia en Productos y Procesos de Córdoba (CEPROCOR), Ministerio de Ciencia y Tecnología, Pabellón CEPROCOR, CP 5164, Santa Maria de Punilla, Córdoba, Argentina

Received February 13, 2008; Revised Manuscript Received September 2, 2008

ABSTRACT: In the present work we develop a Monte Carlo study of polyelectrolyte adsorption on a charged surface by means of a primitive model for the PE and the ions; the small ions are simulated in the Grand Canonical ensemble. Free energy profiles for the adsorption process were obtained using a generalization of Jarzynski equality, where a minimum was found close to surface. This minimum stems from a balance between the loss of configurational entropy by the PE chain upon adsorption, and the gain of translation entropy caused by the release of small ions. The results of the free energy of adsorption are compared with those from a previous work using mean field equations and simulated density profiles.

1. Introduction

Polyelectrolytes (PEs) are linear chain polymers that in solution may have a charge on their monomers. Aqueous PEs solutions, in the presence or absence of other small ions, show a number of remarkable physicochemical properties.[1] Furthermore, many molecules like DNA that play key roles in biology exhibit this type of behavior and can be considered to be PEs.[1] For this reason, gaining further insight into the molecular mechanisms that lead to these properties are of primarily importance both, for understanding polyelectrolyte behavior, and for applying them potentially to technological purposes.

The property that we intend to address in the present work is the free energy of adsorption of PEs on charged surfaces. Numerous experimental studies have focused on the structural characteristics of the adsorbed polyelectrolyte and its stability upon changes in its environmental conditions like temperature and ionic strength of the solution.[2] From a simplistic electrostatic analysis, it could be concluded that PE adsorption on an oppositely charged surface should have a natural limit when the original surface charge is completely compensated by the charge density of the adsorbed chains (charge compensation). However, under certain circumstances the amount of PE adsorbed is found to be larger than that required to compensate the surface charge,[2] so that a surface charge density with a charge opposite to that of the original surface is generated. This phenomenon is called charge reversal, which may be of such an extent that the magnitude of the final charge density is equal to the original one. Then, the adsorbed layer of PE could be placed in the presence of another PE of opposite charge, to yield again a surface with charge overcompensation. Performed cyclically, this is the process employed to generate PE multilayers.[2] The structure and properties of these multilayers as well as technological applications are multiple,[2] and depend on the conditions under which they are generated, like charge density of the substrate, ionic strength, etc. A special case observed for the first time in the work of Perez et al.[3,4] is the generation of self-assembled polyelectrolyte nanorings using polyelectrolytes. They are formed by poly(ethylenimine) (PEI) and poly(sodium 4-styrenesulfonate) (PSS) during the first two steps of the formation of the self-assembled polyelectrolyte films (SAPFs).

Numerous theoretical studies[5−11] and computer simulations[12−19] have been undertaken to understand the phenomenon of PE adsorption and the related problems of charge reversal and overcompensation. In ref 5, a theoretical approach was developed on the basis of numerical studies of mean field equations. From this model, the concentration profile of the PEs can be explicitly calculated. Nonlinear effects, like ion condensation on the PE and the substrate surface, are usually ignored. Furthermore, many studies are restricted to relatively low electrostatic potentials, where the Debye−Hückel approximation can be safely employed to deal with electrostatic interactions. In refs 6−11, the adsorption of PEs was studied using different boundary conditions. Computer simulations have been carried out using Monte Carlo,[12−15] molecular dynamics[16−18] and Brownian dynamics.[19] Messina[15] performed Monte Carlo simulations of PE adsorption in the canonical ensemble, in the absence of a foreign salt. He found that an extra (nonelectrostatic) additional field is required to enhance the stability of the adsorbed PE and produce significant charge overcompensation.

Experimental and simulations studies focusing on the thermodynamic aspects of polyelectrolyte adsorption[20−26] are far less frequent than those concerned with structural aspects. Free energy is a fundamental descriptor of polyelectrolyte adsorption, and calculation of free energy differences is essential for the understanding of these processes. In a previous study[27] we have focused on the electrostatic aspects of the adsorption thermodynamics of polyelectrolytes on charged surfaces, performing specific calculations of the relative enthalpic and entropic contributions from grand canonical Monte Carlo simulations. Mean field equations were applied to density profiles obtained from the simulations in order to assess the entropic contributions. The results suggest that these are the driving force for this phenomenon, which stems from the release of counterions from the double layers of the PE and the charged surface. The positive enthalpy value was rationalized in terms of the decrease in the number of ionic pairs upon adsorption. Although the model was rather simplistic to be directly applied to experimental systems, it put forward new viewpoints on the PE adsorption on charged surfaces. These concepts may also be helpful to interpret results

* Corresponding author. E-mail: eleiva@fcq.uncor.edu.
[†] Unidad de Matemática y Física, Facultad de Ciencias Químicas, Universidad Nacional de Córdoba, INFIQC.
[‡] Centro de Excelencia en Productos y Procesos de Córdoba (CEPROCOR), Ministerio de Ciencia y Tecnología, Pabellón CEPROCOR.

10.1021/ma800325e CCC: $40.75
Published on Web 10/14/2008

concerning the interaction of polyelectrolytes with lipid structures[28] and colloids.[29,30]

The mean field calculations were useful to discriminate between the enthalpic and entropic contributions to the process; however, a more rigorous calculation of the free energy is still desirable. The traditional equilibrium methods used for this purpose, e.g. thermodynamic integration,[31] have been recently extended to a nonequilibrium method based on Jarzynski equality (JE):[32,33]

$$\langle e^{-\beta W} \rangle = e^{-\beta \Delta F} \quad (1)$$

This theorem relates the work performed on a system during a nonequilibrium process to the free energy difference between two equilibrium states of that system. The angular brackets denote an average over an ensemble of realizations (repetitions) of a thermodynamic process, during which a system evolves while a control parameter λ is varied from an initial λ_{init} to a final value λ_{fin}. Thus, W is the external work performed on the system during the realization of one of the processes; $\Delta F = F_{fin} - F_{init}$ is the free energy difference between two equilibrium states of the system, corresponding to $\lambda = \lambda_{init}$ and $\lambda = \lambda_{fin}$; $\beta = 1/(k_b T)$ is the inverse temperature, where k_b is Boltzmann's constant and T is the temperature of the heat bath with which the system is equilibrated prior to the start of each realization of the process. Jarzynski equality has been verified experimentally[34] by stretching single RNA molecules; its computational application is described in references.[35−37]

In this work we perform a Monte Carlo (MC) simulation applying a generalization of JE to the study of PE adsorption on a charged surface by means of a primitive model for the PE and the ions. In the following section, we present the computational methods. The results of the free energy values obtained with JE and compared with those from mean field equations are shown in section 3. Finally, concluding remarks and perspectives are given in section 4.

2. Computational Methods

2.1. Computational Model. We use a primitive model for monomers and ions. The solvent is modeled in terms of a dielectric continuum, i.e., an implicit solvent with relative dielectric constant $\varepsilon_r = 78$. The polyelectrolyte is modeled as a flexible chain of positively charged spheres with a diameter of $d = 0.4$ nm. Two consecutive monomers in each chain are connected by a harmonic stretching spring whose potential is taken to be $u_{bond} = k_{eq}(l - l_0)^2$, where l is the bond length and $l_0 = 0.5$ nm is the equilibrium bond length. The spring constant $k_{eq} = 1000 k_b T/\text{nm}^2$ is chosen to be high enough to prevent fluctuations of the bond length.

The simulation box is a rectangular one of dimensions $W \times W \times L$. Periodic boundary conditions are applied in the x and y directions, with hard walls at $z = 0$ and $z = L$. The wall at $z = 0$ has a negatively surface charge density σ_s, uniformly distributed. The polyelectrolyte is made of N_p PE chains, each with N_m monomers. The number of free ions of the system was adjusted automatically by means of a grand canonical MC (GCMC) procedure.

All the small ions of the system are considered to be rigid spheres with a diameter of $d = 0.4$ nm with an embedded unit (positive or negative) charge. Since the charge density at the $z = 0$ wall is assumed to be negative, its counterions are positive. In the absence of PE, this wall has N_{cs} counterions, with $N_{cs} = |\sigma_s| \times W^2$. A free (nonadsorbed) PE chain has $N_m \times f$ counterions, where f is the fraction of charged monomers in the PE ($f = 1$ in this work), yielding a total number of $N_{cp} = N_p \times N_m \times f$ counterions when all the PE chains are free and noninteracting.

In a simulation, where all the constituents of the system are present, the number of positive N_i^+ and negative N_i^- ions will be given by $N_i^+ = N_{cs} + N_s^+$ and $N_i^- = N_{cp} + N_s^-$, where $N_s^+ = N_s^-$ is the total number of ion pairs introduced in (removed from) the system because of the GCMC procedure.

As indicated above, the grand canonical ensemble is the natural choice to study PE adsorption on a charged surface. For a given bulk electrolyte concentration, the chemical potential of the electrolyte species is unambiguously determined and this is the chemical potential applied to our model system. In the present work, the bulk electrolyte concentration was 0.01 M.

This situation is very close to the experimental one, where a large amount of electrolyte in the system maintains the activity of ions practically unaltered upon polyelectrolyte adsorption or desorption. The procedure adopted to carry out the GCMC simulation was very similar to that prescribed by Torrie and Valleau.[38]

The potential energy of the system is a sum over pair interactions between the particles of the system and single particle interactions with the wall. The pair interactions are assumed to be electrostatic and of the hard-sphere type according to:

$$u(\vec{r}_{ij}) = \frac{Z_i Z_j e^2}{4\pi\varepsilon_0\varepsilon_r r_{ij}}, \quad r_{ij} > d$$
$$u(\vec{r}_{ij}) = \infty, \quad r_{ij} \le d \quad (2)$$

where Z_i is the charge of the particle (ion of monomer), e is the elemental charge, $\varepsilon_0\varepsilon_r$ is the permittivity of the dielectric continuum, $\vec{r}_{ij}$ is the relative position vector, $r_{ij} = |\vec{r}_{ij}|$ is the distance between particles i and j. The interaction between particle i and the wall is given by:

$$u(z_i) = \frac{\sigma_s Z_i e z_i}{2\varepsilon_0\varepsilon_r}, \quad d/2 < z_i < L - d/2$$
$$u(z_i) = \infty, \quad d/2 \ge z_i \text{ or } z_i \ge L - d/2 \quad (3)$$

where z_i is the z coordinate of position r_i of the particle i, and σ_s is the surface charge density of the charged wall.

Different types of methods are available for the calculation of the electrostatic potential energy of a finite sample in a computer simulation. One of them is the Ewald method (or related ones),[31] where a part of the interaction energy is summed in real-space and another one in reciprocal-space.[31] The so-called external potential method (EPM), as first proposed by Torrie and Valleau[38] and subsequently modified by Henderson et al.[39] constitutes an alternative method to deal with the long-range electrostatic interactions. This technique takes into account that the interaction of a charged particle with the replicas of the simulation cell is approximately dipolar in nature and, for a double layer system, it will attract the central cell counterions toward the surface. If Ewald-type lattice sums appropriate to the slab geometry were used to account for this effect, then the spurious periodicity, originally devised to minimize finite-system effects arising from the long-range forces, would be explicitly introduced into the long-range force part of the Hamiltonian. This would result in an unphysical correlation between the fluctuations of the charge distribution in the surrounding cells and those in the central cell. A more realistic imitation of the energy change associated with a change in the position of a particle in a nonperiodic infinite system was obtained by Torrie and Valleau[38] by taking for the surroundings of the central cell a charge distribution given by the average charge distribution of the central box as measured over all preceding configurations. In this approach, the influence of the lateral charges on the central cell is accounted for by infinite sheets parallel to the charged walls. In Henderson's algorithm,[39] each ion has its own sheet at the same z coordinate as the particle. The charged sheet

corresponding to each ion carries a uniform charge density of $Z_i e/W^2$ where $Z_i e$ is the charge of the central ion. Each particle interacts with each sheet, minus the square hole corresponding to the central particle in which the interaction is taken into account explicitly by the intermolecular potentials. The potential energy of an ion $Z_i e$ above the center of a charged sheet of dimension $W' \times W'$ corresponding to an ion $Z_j e$ is

$$u_{i,csh}(z_i, z_j, W') = \frac{Z_i Z_j e^2}{4\pi\varepsilon_0\varepsilon_r W'^2}\int_{-W'/2}^{W'/2}\int_{-W'/2}^{W'/2}\frac{\mathrm{d}x\,\mathrm{d}y}{r}$$

where the vector $r = (x,y,z_i - z_j)$ points from de unit area of the sheet to the particle. By performing the integration, we obtain:

$$u_{i,csh}(z_i, z_j, W') = \frac{Z_i Z_j e^2}{4\pi\varepsilon_0\varepsilon_r W'^2}\left\{4T\ln\left(\frac{0.5 + r_1}{r_2}\right) - |z|\left[2\pi - 4\arctan\left(\frac{4|z|r_1}{W'}\right)\right]\right\}$$

where $|z| = |z_i - z_j|$ is the distance between a particle and a sheet, $r_1 = [0.5 + (z/W')^2]^{1/2}$ and $r_2 = [0.25 + (z/W')^2]^{1/2}$. In the limit of $W' \to \infty$ the value of the function is $u_{i,csh}(z,\infty) = [-Z_i Z_j e^2/(2\varepsilon_0\varepsilon_r W^2)]|z|$. The total energy of the ions in the central cell with the external charge distribution of the system is given by:

$$u_{EPM} = \sum_{i=1}^{N}\sum_{j=1}^{N}[u_{i,csh}(z_i, z_j, \infty) - u_{i,csh}(z_i, z_j, W)]$$

The term in brackets represents the electrostatic interaction of particle i with the images of particle j outside the simulation box. These images are represented as an infinite sheet with a square hole of dimensions $W \times W$.

In the present approach, we ignore the problem of image forces. This has been considered by Messina in previous work,[14] where it has been demonstrated that image forces may reduce the degree of polyelectrolyte adsorption, but with the finding that overcharging is robust against image forces. Thus, leaving aside image charges may lead to an overestimation (in absolute value) of the free energies of adsorption. However, image charge effects appear to become smaller the larger the chain of the PE, so that we expect that for the present chain length our results should be qualitatively correct. On the other hand, we consider explicitly the salt-containing environment and make a comparison with the results of the mean-field approximation.

In addition to ion pair removal and insertion, system equilibration was achieved taking into account motion of single particles, translation of the PE chain with its condensed ionic atmosphere, pivot motion of the PE, and flip motion of the chains.[40]

The relevant quantities measured in the simulation are the concentration profiles of single cations, single anions and PE as a function of the distance from the charged surface. These quantities are denoted as $\rho_+(z)$, $\rho_-(z)$, and $\rho_{Poly}(z)$ respectively. They were calculated using the standard histogram procedure. The center of mass of the polyelectrolyte chain is defined according to:

$$R_{cm} = \frac{1}{N_m}\sum_{i=1}^{N_m} r_i \tag{4}$$

The z component of R_{cm} is

$$z_{cm} = \frac{1}{N_m}\sum_{i=1}^{N_m} z_i \tag{5}$$

Histograms were constructed from the z_{cm} values obtained along the simulation, defining the probability density $\rho_{CM}(z_{cm})$.

Note that the density $\rho_{Poly}(z)$ can be interpreted as the monomer concentration as a function of the distance from the surface of the substrate, while $\rho_{CM}(z_{cm})$ corresponds to the probability of finding the center of mass of the polymer at a given distance from the surface. These two quantities are related by the following equation:

$$N_m\int \mathrm{d}V\,\rho_{CM}(z_{cm}) = \int \mathrm{d}V\,\rho_{Poly}(z) \tag{6}$$

The electrostatic potential $\psi(z)$ was calculated in turn from the total charge density $\rho(z) = \rho_+(z) - \rho_-(z) + \rho_{Poly}(z)$ via the equation:

$$\psi(z) = -\frac{e}{\varepsilon_0\varepsilon_r}\int_z^L [\rho(z')(z' - z)]\,dz' \tag{7}$$

As a reference for the electrostatic potential, we have taken $\psi(L) = 0$.

The results of the simulations with charged surfaces in the absence of PE were compared with the solution of the Poisson−Boltzmann equation[41] in order to check the performance of the procedure developed and a good agreement was obtained.

2.2. Calculation of the Free Energy of the PE Adsorption Process. Free energy changes were calculated between an initial and a final state defined according to the considerations given below. As initial state, we consider a situation where the PE is located at a point away from the surface where the overlap between the double layers of the surface and the PE becomes negligible within the accuracy of our calculation. The final state is less straightforward to define. Below we will attempt a definition in terms of the center of mass of the polyelectrolyte chain.

Under canonical conditions, the equilibrium free Helmholtz energy difference ΔF between two states characterized by the Hamiltonians H_{init} and H_{fin} is given by:

$$\mathrm{e}^{-\beta\Delta F} = \frac{Q_{fin}}{Q_{init}} = \frac{\int \mathrm{d}\Gamma\,\mathrm{e}^{-\beta H_{fin}(\Gamma)}}{\int \mathrm{d}\Gamma\,\mathrm{e}^{-\beta H_{init}(\Gamma)}} \tag{8}$$

where $\Gamma \equiv (p,q)$ denotes a point in the $6 - N$ dimensional space (N being the number of particles), and Q_{init}, Q_{fin} are the partition functions corresponding to H_{init}, H_{fin}, respectively.

The typical method of computing this difference is via thermodynamic integration,[31] where the free energy change is written as

$$\Delta F = \int_{\lambda_{init}}^{\lambda_{fin}} \mathrm{d}\lambda \left\langle\frac{\partial H(\lambda)}{\partial\lambda}\right\rangle_\lambda \tag{9}$$

where the brackets denote an ensemble average. This type of integration has been described in the literature.[31] That is, the derivative is calculated in a number of simulations and its average is integrated by some proper numerical method like Gaussian quadrature. Wallin and Linse have used this type of method along with Monte Carlo simulations to study the adsorption of polyelectrolytes on charged micelles.[24−26] These authors obtained structural data on the micelle-polyelectrolyte complex and thermodynamic quantities for the complexation as a function of chain flexibility,[24] the polyelectrolyte linear charge density[25] and the surfactant tail length.[26] They noted that ion release after polyelectrolyte adsorption on the micelle is an important factor for the process.

2.2.1. Jarzynski Equality. Since eq 9 involves simulations for equilibrium states, the procedures turn to be rather computational time-consuming. However, Jarzynski has shown that the free energy difference of eq 8 is related to a nonequilibrium average.[32,33] In the path integral notation, the Jarzynski equality can be written as[42]

$$e^{-\beta\Delta F} = \int \boldsymbol{D}\Gamma_\tau \boldsymbol{P}(\Gamma_\tau) e^{-\beta W(\tau)} = \langle e^{-\beta W(\tau)} \rangle_0 \quad (10)$$

where $\int \boldsymbol{D}\Gamma_\tau$ denotes an integration over all possible trajectories in phase space and Γ_τ denotes a particular trajectory. $\boldsymbol{P}(\Gamma_\tau)$ is the statistical weight functional of the trajectory Γ_τ that includes the canonical distribution of the initial conditions.[42] Assuming that an external perturbation is applied to H_{init} and switches the system to H_{fin} at τ_{steps} steps, the step-dependent Hamiltonian is now parametrized by a function $\lambda(\tau)$ in such a way that $H[\lambda(0)] = H[\lambda_{init}] \equiv H_{init}$ and $H[\lambda(\tau_{steps})] = H[\lambda_{fin}] \equiv H_{fin}$. It must be noted that the process is not conservative since work is done on the system.

The work done on the system is given by

$$W(\tau') = \int_0^{\tau'} d\tau\, \dot{\lambda} \frac{\partial H[\lambda(\tau)]}{\partial \lambda} \quad (11)$$

where $\dot{\lambda} = (d\lambda)/(d\tau)$.

When the switch between the initial and the final state is undertaken at a finite rate, the work W may take different values with a probability $g(W)$. Thus, the average work may be written as $\langle W \rangle = \int_{-\infty}^{\infty} dW\, g(W) W$ and the Jarzynski equality becomes $e^{-\beta\Delta F} = \int_{-\infty}^{\infty} dW\, g(W) e^{-\beta W}$. In the limit of a reversible process, $g(W) \rightarrow \delta(W - \Delta F)$ and the work done on the system is given by eq 9.

2.2.2. The Stiff-Spring Approximation. For the present purposes, a potentially rewarding application of the Jarzynski equality is the calculation of the free energy profile of a polyelectrolyte approaching a charged surface, which corresponds to the potential of mean force (PMF).[43] In order to proceed, we need to define a reaction coordinate along which adsorption proceeds in the configuration space. This reaction coordinate describes the advance of the adsorption process. The natural choice for the reaction coordinate is the distance of center of mass of PE to the charged surface, z_{cm}, as defined in eq 5. When the z-component of the center of mass of PE has the value $z_{cm} = \lambda_{cm}$, the PMF $\Omega(\lambda_{cm})$ is given through the following Botzmann-weight average over all degrees of freedom other than the reaction coordinate:[35,36]

$$\exp[-\beta\Omega(\lambda_{cm})] = \int d\Gamma\, \delta(z_{cm} - \lambda_{cm}) \exp[-\beta H(\Gamma)] \quad (12)$$

In order to apply JE to the calculation of $\Omega(\lambda_{cm})$, we need to define an external parameter λ_{cm} that must be related to z_{cm} through a driving potential $h_\lambda(\Gamma(\tau))$. This will be formed as follows:

$$h_\lambda(\Gamma(\tau)) = k(z_{cm} - \lambda_{cm})^2 \quad (13)$$

in order to maintain the position of center of mass of the PE close to the value λ_{cm}, where k is a spring force constant. The parameter k must be chosen in such a way as to obtain a small statistical noise and an adequate matching of the different degrees of freedom to the motion of the center of mass. This selection depends on the rate at which the system is driven from the initial to the final state. We found that $k = 10 k_b T/\text{nm}^2$ is a suitable value for the simulation conditions described below. The Hamiltonian of the new system is the following:

$$\tilde{H}_\lambda(\Gamma(\tau)) = H(\Gamma(\tau)) + h_\lambda(\Gamma(\tau)) \quad (14)$$

The parameter λ_{cm} was changed from $\lambda_{init} = 30$ nm to $\lambda_{fin} = 0$ nm, according to the law $\lambda_{cm} = \lambda_{init} + \upsilon\tau$, with $\upsilon = (\lambda_{fin} - \lambda_{init})/\tau_{steps}$, where τ_{steps} was 100000.

According to the previous definitions, the work along each trajectory is given by

$$W = 2k\upsilon \int_0^{\tau_{steps}} d\tau\, (z_{cm} - \lambda_\lambda) \quad (15)$$

Applying JE to the $\tilde{H}$-system during the step interval between zero and τ we obtain:

$$\tilde{F}_\tau - \tilde{F}_{init} = -\frac{1}{\beta} \log\langle \exp[-\beta W(\tau)] \rangle \quad (16)$$

Here $\tilde{F}$ is the Helmholtz free energy of the $\tilde{H}$-system, given by

$$\exp(-\beta \tilde{F}_{\lambda_{cm}}) = \int d\Gamma \exp(-\beta \tilde{H}_{\lambda_{cm}}(\Gamma(\tau))) \quad (17)$$

We have obtained a formula for the free energy $\tilde{F}$ of the $\tilde{H}$-system, but what we actually attempt to determine is the PMF Ω of the original H-system. The free energy $\tilde{F}$can be written in terms of the PMF Ω as follows:

$$\begin{aligned} \exp(-\beta \tilde{F}_{\lambda_{cm}}) &= \int d\Gamma \exp[-\beta H(\Gamma) - \beta k(z_{cm} - \lambda_{cm})^2] \\ &= \int d\Gamma \int d\lambda'_{cm}\, \delta(z_{cm}(\mathbf{r}) - \lambda'_{cm}) \times \exp[-\beta H(\Gamma) - \beta k(z_{cm} - \lambda_{cm})^2] \\ &= \int d\lambda_{cm} \exp[-\beta\Omega(\lambda_{cm}) - \beta k(z_{cm} - \lambda_{cm})^2] \end{aligned} \quad (18)$$

If k is large enough (this is fulfilled in the present simulations with the selection $k = 10 k_b T/\text{nm}^2$), the larger contribution of the argument in eq 18 to the integral will be given for z_{cm} values close to λ_{cm}, so we can approximate:

$$\tilde{F}_{\lambda_{cm}} \approx \Omega(\lambda_{cm})$$

For the sampling paths, we selected initial configurations from an ensemble of trajectories generated after 10^6 MC equilibration steps with z_{cm} fixed at 30 nm.

2.2.3. Jarzynski Relation in a Grand Canonical Monte Carlo Simulation. All the previous discussion was given within the canonical ensemble, which is the environment from which the JE was originally derived. However, since we are simulating a finite system and intent to represent a situation where the region close to the surface is coupled to a bulk electrolyte, grand canonical conditions were set for the electrolyte. Thus, rather than using eq 10, we employed its generalization for grand canonical conditions as provided by Schmiedl and Seifert[44] shown below. For the present system, the relationship between the grand canonical partition function Ξ and the grand canonical potential J leads to the relationship:

$$\begin{aligned} e^{-\beta\Delta J} &= \frac{\Xi_{fin}}{\Xi_{init}} \\ &= \frac{\sum_{N^+}\sum_{N^-} \int d\Gamma\, e^{-\beta H_{fin}(\Gamma)} e^{\beta N^+ \mu_+} e^{\beta N^- \mu_-}}{\sum_{N^+}\sum_{N^-} \int d\Gamma\, e^{-\beta H_{init}(\Gamma)} e^{\beta N^+ \mu_+} e^{\beta N^- \mu_-}} \\ &= \frac{\sum_{N^+}\sum_{N^-} Q_{fin}(N^+, N^-, V, T) e^{\beta(N^+\mu_+ + N^-\mu_-)}}{\sum_{N^+}\sum_{N^-} Q_{init}(N^+, N^-, V, T) e^{\beta(N^+\mu_+ + N^-\mu_-)}} \end{aligned} \quad (19)$$

where J is the grand canonical potential[44] given by

$$J = U - TS - \sum\nolimits_j \mu_j n_j \quad (20)$$

A generalization of JE to grand canonical equilibrium conditions has been given by Schmiedl and Seifert:[44]

$$\langle e^{-\beta[W - \Delta(\sum_j \mu_j n_j)]} \rangle = e^{-\beta\Delta J} \quad (21)$$

Thus, in addition to the calculation of the work W as described above, the change in the number of particles was monitored along each trajectory and included in the average on the lhs of

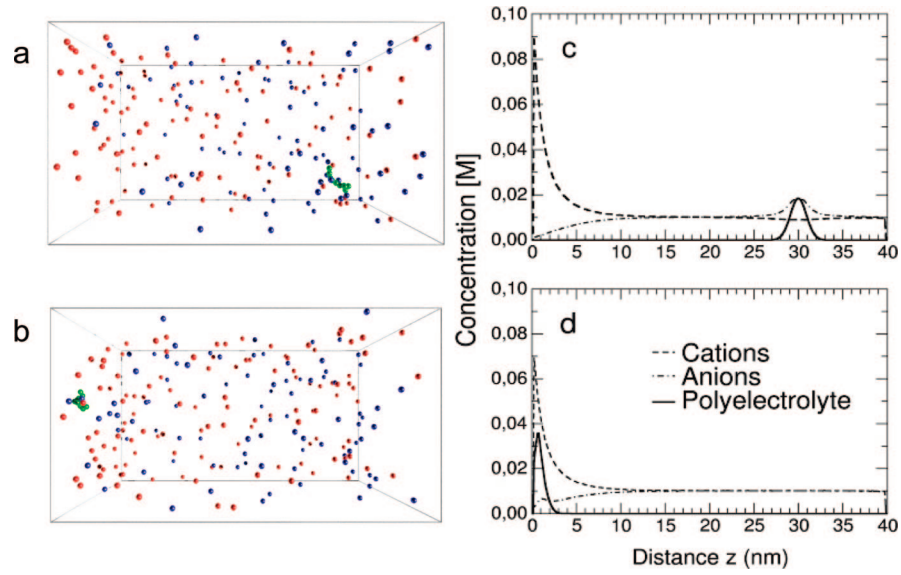

Figure 1. Sample configurations of a simulation of the adsorption of a 10-monomer PE chain on a charged surface. (a) PE far from the charged surface. (b) PE close to the charged surface. Concentration profiles corresponding to the simulations illustrated in parts a and b are shown in figures c and d respectively. The resulting surface monomer density was 0,025 monomers/nm^2. The surface charge density was $\sigma_s = -0.1$ e/nm^2. The bulk electrolyte concentration was $c = 0.010$ M. Green: polyelectrolyte monomers. Red: negative ions. Blue: positive ions.

eq 21. In the grand canonical ensemble the force mean potential $\Omega^{GC}(\lambda_{cm})$ can be written as

$$\exp[-\beta\Omega^{GC}(\lambda_{cm})] = \sum_{N^+}\sum_{N^-}\int d\Gamma\ \delta(z_{cm} - \lambda_{cm})e^{-\beta H(\Gamma)}e^{\beta N^+\mu_+}e^{\beta N^-\mu_-} \quad (22)$$

3. Results

3.1. Concentration Profiles. Parts a and b of Figure 1 show the simulation box, where the charged surface is located at the left side, with some sample configurations during the adsorption process of a 10-monomer PE chain, starting from a point far away from the surface (Figure 1a) and ending with the adsorption of the PE on it (Figure 1b). Accordingly, parts c and d of Figure 1 show the concentration profile of the PE far from, and close to the charged surface respectively. From the last two figures, it can be seen that the negatively charged surface induces an excess of small positive ions and a depletion of small negative ions. This is the usual electrical double layer.[41] It can also be noticed that the PE is surrounded by a compact layer of negative ions, corresponding to the Manning condensation[45,46] phenomenon. In parts b and d of Figure 1, two remarkable phenomena are also evident: (i) the PE chain becomes confined close to the wall, loosing degrees of freedom perpendicularly to the surface, with the concomitant loss of configurational entropy; (ii) most of the ions conforming the ionic atmosphere of the PE and that of the surface are released, i.e., the PE replaces most of its counterions by the charge of the surface, and a similar phenomenon occurs with the counterions of the surface, which suggests, an efficient ionic exchange under the present simulation conditions.

3.2. Work and Free Energy Calculations. Figure 2a shows the values for the change in the number of particles $\Delta N = \Delta N^+ + \Delta N^-$, the work W and the quantity $W - \Delta(N^+\mu_+ + N^-\mu_-)$ for a typical simulation path. Figure 2b presents $W - \Delta(N^+\mu_+ + N^-\mu_-)$ results for simulations with of a 10-monomer chain, with $\sigma = -0.10e$/nm^2 for 10 different paths. The dispersion calculated from 40 different trajectories is found to be below $1.5k_bT$. From these profiles we note that close to the surface all values are negative, denoting the spontaneous nature of the adsorption process. A minimum becomes evident around $z_{cm} \approx$ 1.00 nm. The free energy profiles of PE adsorption were obtained by the application of eq 21 to profiles similar to those shown in Figure 2a.

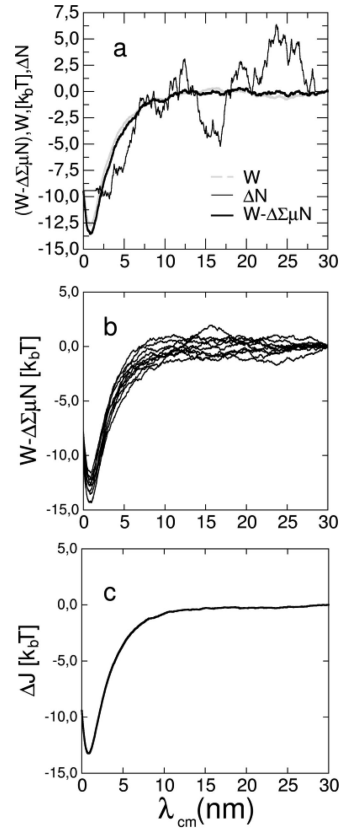

Figure 2. Adsorption of a PE chain made of 10 monomers on a charged surface with$\sigma_s = -0.10e$/nm^2 (a) Profiles for the work W, the change in the number of particles ΔN and the quantity $W - \Delta(N^+\mu_+ + N^-\mu_-)$ for a typical realization of the adsorption process. (b) $W - \Delta(N^+\mu_+ + N^-\mu_-)$ profiles for 10 different trajectories. (c) ΔJ profile obtained from 40 different trajectories.

Free energy profiles for PE adsorption similar to those shown in Figure 2a, but at different surface charges are shown in Figure 3. For an uncharged surface, the free energy increases mono-

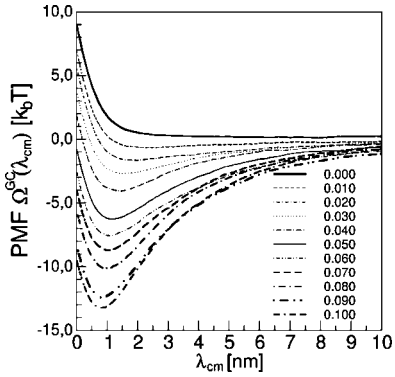

Figure 3. Free energy profiles for the adsorption of polyelectrolyte chain made of 10 monomers at different negative surface charges densities (in e/nm^2). Absolute values are reported in the figure.

tonically as the surface is approached. This process is not spontaneous since the loss of configurational entropy by the PE is not balanced by the entropy increase due to the release of counterions. On the other hand, for the other surface charge densities, a minimum appears, whose depth increases and approaches the surface as the surface charge density becomes more negative.

Simulations were also performed without the application of any constrain to z_{cm}, allowing for the spontaneous evolution of the system to its equilibrium configuration. The concentration of the PE and that of the small ions are shown as a function of the distance from the charged surface in Figure 1d. The probability density of finding the center of mass $\rho_{cm}(z_{cm})$ at a given distance from the charged surface was also calculated, as plotted in Figure 4 for three different surface charge densities. This probability density is closely related to the potential of mean force. To show this, we begin with the probability density $\rho(\Gamma)$ of finding the system at the point Γ:

$$\rho(\Gamma) \propto \frac{e^{-\beta H(\Gamma)} e^{\beta N^+ \mu_+} e^{\beta N^- \mu_-}}{\Xi} \tag{23}$$

The probability density $\rho_{cm}(\lambda_{cm})$ of finding the center of mass at the distance $\lambda_{cm}(z_{cm} = \lambda_{cm})$ can be obtained integrating eq 17 according to

$$\rho_{cm}(\lambda_{cm}) \propto \frac{\sum_{N^+}\sum_{N^-}\int d\Gamma\ \delta(z_{cm}(\Gamma) - \lambda_{cm}) e^{-\beta H(\Gamma)} e^{\beta N^+ \mu_+} e^{\beta N^- \mu_-}}{\Xi} \tag{24}$$

On the other hand, we can rewrite the grand canonical partition function in terms of the potential of mean force according to:

$$\begin{aligned}\Xi &\propto \sum_{N^+}\sum_{N^-}\int d\Gamma\ e^{-\beta H(\Gamma)} e^{\beta N^+ \mu_+} e^{\beta N^- \mu_-} \\ &\propto \int d\lambda_{cm} \sum_{N^+}\sum_{N^-}\int d\Gamma\ \delta(z_{cm}(\Gamma) - \lambda_{cm}) e^{-\beta H(\Gamma)} e^{\beta N^+ \mu_+} e^{\beta N^- \mu_-} \\ &\propto \int d\lambda_{cm} \exp[-\beta \Omega^{GC}(\lambda_{cm})]\end{aligned} \tag{25}$$

So, by replacing (19) in eq 18m we obtain:

$$\rho_{cm}(\lambda_{cm}) = \frac{\exp[-\beta \Omega^{GC}(\lambda_{cm})]}{\int d\lambda_{cm} \exp[-\beta \Omega^{GC}(\lambda_{cm})]} \tag{26}$$

where the relationship between the probability density $\rho_{cm}(\lambda_{cm})$ and $\Omega^{GC}(\lambda_{cm})$ becomes evident. This relationship is very useful to test the precision of the calculations, since we can compare the prediction of this equation using the $\Omega^{GC}(\lambda_{cm})$ obtained with generalized JE (see Figure 3) with

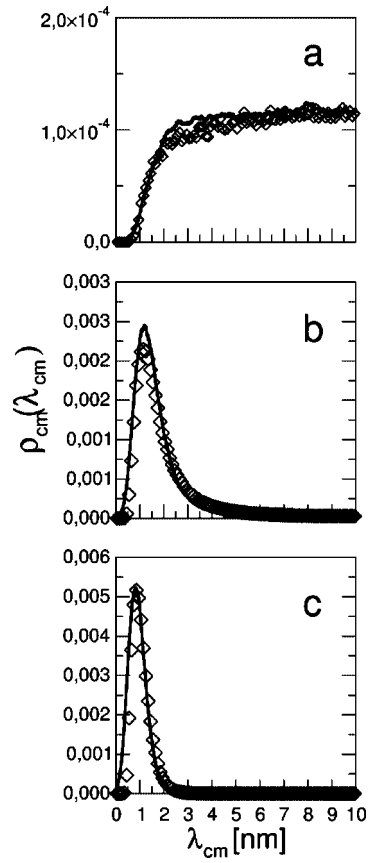

Figure 4. Probability density of finding the center of mass $\rho_{cm}(z_{cm})$ at a given distance from the charged surface for different charges densities: (a) $\sigma_s = 0.00e$/nm^2; (b) $\sigma_s = -0.05e$/nm^2; (c) $\sigma_s = -0.10e$/nm^2. The continuous lines denote the prediction made according to eq 26 using the potential of mean force $\Omega^{GC}(\lambda_{cm})$ obtained with Jarzynski equality, while the symbols are the results from unbiased Monte Carlo simulations.

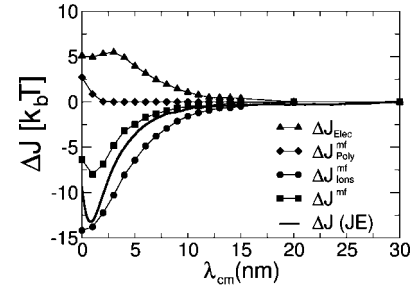

Figure 5. Comparison between the free energy profiles obtained using generalized Jarzynski equality over a set of 40 trajectories (full line) and the mean the field approximation, ΔJ^{mf}(squares). The different contributions to $\Delta J^{mf}(\lambda_{cm})$ are also shown as a function of the distance from the charged surface. $\Delta J_{poly}{}^{mf}$ is the contribution due to the configurational changes of the polyelectrolyte chain, $\Delta J_{ions}{}^{mf}$ is the translational contribution of the small ions, and ΔJ_{elec} is the electrostatic contribution. $\sigma_s = -0.10e$/nm^2.

the profiles $\rho_{cm}(\lambda_{cm})$ obtained from a current (unbiased) Monte Carlo calculation.

This comparison is drawn in figure 4 for three different charge densities, namely $\sigma_s = 0e$/nm^2 (Figure 4a), $\sigma_s = -0.05e$/nm^2 (Figure 4b) and $\sigma_s = -0.10e$/nm^2 (Figure 4c), where a reasonable good agreement is found.

It is interesting to compare the free energy profiles calculated in this work through the generalized JE with mean field predictions (Figure 5), where the different entropic contributions (polyelectrolyte, small ions) to the free energy profile can be

discriminated. In order to obtain the mean field free energy values, simulations were performed with the center of mass of the polyelectrolyte fixed at a given distance λ_{cm} from the charged wall by means of a harmonic spring (see eq 13). As in our previous work,[27] the concentration profiles of the participating species were then calculated at each λ_{cm} and mean field equations were used. Within the mean field approximation, the free energy of the system can be written as a sum of three contributions:[5]

$$\Delta J^{mf}(\lambda_{cm}) = \Delta J^{mf}_{poly} + \Delta J^{mf}_{ions} + \Delta J_{elec} \tag{27}$$

where ΔJ_{elec} denotes the contribution from the electrostatic interactions in the system that is calculated straightforwardly from the simulation through $\Delta J_{elec} = \langle U_\lambda \rangle - \langle U_{30\text{nm}} \rangle$. $\Delta J_{poly}{}^{mf}$ and $J_{ions}{}^{mf}$ indicate the nonelectrostatic contributions from the polyelectrolyte (configurational) and the small ions (translational) respectively.

According to the mean field approximation, $J_{poly}{}^{mf}$ can be written as[5]

$$J^{mf}_{poly} = k_b T \int \left[\frac{a^2}{6} |\nabla \varphi|^2 + \frac{1}{2} \nu \varphi^4 \right] \mathrm{d}r \tag{28}$$

where the polymer order parameter $\phi(r)$ is related to the local monomer concentration $c(r)$ via the relationship $c(r) = |\phi(r)|^2$ and we refer the free energy to a zero bulk concentration. a is the effective monomer size and ν is the excluded volume contribution, and we have omitted the contribution due to the translational motion of the center of mass of the polymer. The free energy of the small ions $J_{ions}{}^{mf}$ is given by[5]

$$J^{mf}_{ions} = \int \{ k_b T \sum_{i=\pm} [c^i \ln c^i - c^i - c^i_b \ln c^i_b + c^i_b] - \mu^i (c^i - c^i_b) \} \, \mathrm{d}r \tag{29}$$

where $c^i(r)$, $c^i_b(r)$, and $\mu^i(r)$ are the local concentration, the bulk concentration and the chemical potential of the ions $i = \pm 1$, respectively.

Figure 5 shows the different contributions to $\Delta J^{mf}(\lambda_{cm})$ as a function of the distance λ_{cm} for a surface charge density $\sigma_s = -0.10e/\text{nm}^2$. We note that the configurational contribution of the PE, ΔJ^{mf}_{poly}, remains negligible until an approach distance to the surface of 2 nm, where it begins to increase. The electrostatic contribution, ΔJ_{elec}, is always positive and increases upon approach until reaching a maximum around 3 nm. Then it shows a small decrease. These two contributions discourage adsorption. The positive value of ΔJ_{elec} appears at first sight as puzzling. Should not this be negative since the charged polymer is attracted to the oppositely charged surface? To answer this question, we will consider first the situation of a polymer chain before and after adsorption, for the case where charge overcompensation is very small or negligible, so that after adsorption it looses most of its counterion atmosphere. Before adsorption, the system can be considered as consisting of two subsystems. One is made up of the charged surface and its compensating layer of counterions (for the present model made of an excess of positive ions compensating the negative surface charge). The other subsystem can be considered to be the polymer chain, surrounded also by a cloud of negative ions, which compensates its charge. Both interaction energies are negative. Due to the electrostatic screening of the free ions, the two subsystems interact weakly. After adsorption, and with the above assumption of complete charge compensation, the charged surface and the polymer loose their corresponding ionic atmospheres. Since the interaction of the surface with the polymer can be considered roughly similar to the initial interaction of the same surface with its double layer, what has been lost in the system is the interaction energy of the polymer with its ionic atmosphere.

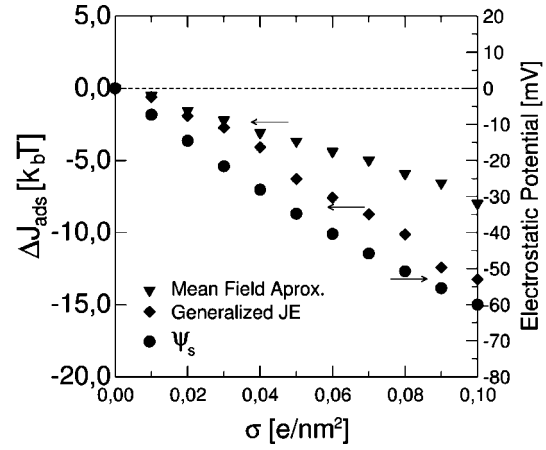

Figure 6. Comparison between the free energy of polyelectrolyte adsorption calculated in the mean field approximation (triangles) and the corresponding values obtained using Jarzynski equality over a set of 40 trajectories (diamonds). The electrostatic potential at the surface is given on the right scale (filled circles on the plot).

As stated above this was a negative quantity. Thus, the total electrostatic energy of the system has increased after polymer adsorption. In the case of charge overcompensation, the polymer does not loose completely its ionic atmosphere upon adsorption, but the situation is similar to the previous one: after adsorption, the positive ionic charge that was initially compensating the negative surface charge is replaced by the polymer plus some of its counterions. Resuming, after adsorption and the concomitant release of counterions, interactions mainly occur between the charged surface and the PE. Therefore, the adsorption process leads to the disappearance of a considerable number of ion pairs, with the consequent energy increase.

The free energy contribution due to small ion release ΔJ^{mf}_{ions} is negative and larger in magnitude than the other two, constituting the driving force of the adsorption process. It is also worth noting that both free energy profiles, the mean field one and that obtained via the JE, show a minimum at about the same approach distances, the minimum of the later being slightly deeper. The balance between the loss of configurational entropy of the polymer upon approach to the surface and the phenomenon of ion release is responsible for the existence of this minimum.

Finally, Figure 6 shows the adsorption free energy of the polymer as a function of the surface charge density within both, the mean field and the JE approximations. The adsorption free energy of the polymer, ΔJ_{ad}, was defined according to the following equation:

$$\Delta J_{ad} = J_{ad} - J_\infty \tag{30}$$

Here J_{ad} is the free energy of the polymer at the minimum of the free energy profiles as seen in figure 3, and J_∞ is the free energy value at a point far from the surface where it is not interacting with the surface. We can observe that the J_{ad} values within both approximations are similar up to a surface charge density of ca. $0.03e/\text{nm}^2$. Then, the difference between the mean field and the JE prediction become more prominent. The coincidence between both approximations at low surface charges is to be expected, since the mean field equations are rigorously valid at low electrostatic potentials, that is, provided the relation $|\beta e \psi_s| < 1$ is fulfilled.[5] For the present system it comes out that the electrostatic potential at the surface $\psi_s = \psi(0)$ (eq 7) is of the order of the thermal energies ($\psi \approx 26$ mV) when the surface charge density is of the order $0.03e/\text{nm}^2$. At larger surface densities, the mean field approximation clearly underestimates the free energy of polyelectrolyte adsorption.

4. Concluding Remarks and Perspectives

In the present work, we have focused on the electrostatic aspects of the adsorption thermodynamics of polyelectrolytes on charged surfaces, for which a rigorous calculation of the potential of mean force by means of Jarzynski equality was performed. Thus, the present work constitutes, to the best of our knowledge, the first attempt to apply this state-of-the art methodology to the problem at hand, which allows for a precise evaluation of the free energy of adsorption for the model proposed. We find a minimum in the PFM originated in the balance between two opposite contributions to the free energy of the system: on one side an increasing one, caused by the loss of configurational entropy of the polymer approaching the wall, and on the other side, a decreasing one, originated by the increase in translational entropy of the small ions due to their release upon polyelectrolyte adsorption. The electrostatic energy increases as the polyelectrolyte chain approaches the wall, but this contribution remains relatively unchanged in the neighborhood of the free energy minimum. A reasonably good agreement is found between the free energy of adsorption computed from the present simulations and the estimations based on a mean field approximation at low surface charges. At high surface charges, the mean field approximation leads to an overestimation of the free energy of adsorption of the polyelectrolyte.

Although at this stage the model is rather simplistic to be applied directly to experimental systems, it puts forward new viewpoints concerning PE adsorption on charged surfaces. Computational models with explicit consideration of the solvent are desirable and will allow discriminating between the present ionic and solvent effects. Before this extension, that will be more demanding computationally, the effect of the change of the electrolyte concentration as well as the formation of polyelectrolyte multilayers needs to be further examined. A related interesting system is the formation of self-assembled polyelectrolyte nanorings, like those found in the work of Perez et al.[3,4]

Acknowledgment. We thank C. Jarzynski for information on the generalization of JE. Financial support from CONICET, Secyt UNC, Program BID1201/OC-AR PICT No. 946 as well as language assistance by Carolina Mosconi are gratefully acknowledged.

References and Notes

(1) *Physical Chemistry of Polyelectrolytes*; Radeva, T., Ed.; Marcel Dekker: New York, 2001.
(2) *Multilayer Thin Films: Sequential Assembly of Nanocomposite Materials*; Decher, G., Schlenoff, J. B., Eds.; Wiley-VCH: Weinheim, Germany, 2003.
(3) Menchaca, J. L.; Flores, H.; Cuisinier, F.; Pérez, E. J. *Phys.: Condens. Matter* **2004**, *16*, S2109−S2117.
(4) Flores, H.; Menchaca, J. L.; Tristan, F.; Gergely, C.; Perez, E.; Cuisinier, F. J. G. *Macromolecules* **2005**, *38*, 521–526.
(5) Borukhov, I.; Andelman, D.; Orland, H. *Macromolecules* **1998**, *31*, 1665–1671.
(6) Varoqui, J. *Phys. II Fr.* **1993**, *3*, 1097–1108.
(7) Borisov, O. V.; Zhulina, E. B.; Birshtein, T. M. *J. Phys. II (Fr.)* **1994**, *4*, 913–929.
(8) Joanny, J. F. *Eur. Phys. J. B* **1999**, *9*, 117–122.
(9) Andelman, D.; Joanny, J. F. *C. R. Acad. Sci. (Paris)* **2000**, *1*, 1153–1162.
(10) Shafir, A.; Andelman, D.; Netz, R. R. *J. Chem. Phys.* **2003**, *119*, 2355–2362.
(11) Muthukumar, M. *J. Chem. Phys.* **1987**, *86*, 7230–7235.
(12) Messina, R. *Macromolecules* **2004**, *37*, 621–629.
(13) Messina, R.; Holm, C.; Kremer, K. *J. Polym. Sci., Part B: Polym. Phys.* **2004**, *42*, 3557–3570.
(14) Messina, R. *Phys. Rev. E* **2004**, *70*−1-9.
(15) Kong, C. Y.; Muthukumar, M. *J. Chem. Phys.* **1998**, *109*, 1522–1527.
(16) Abu-Sharkh, B. *Langmuir* **2006**, *22*, 3028–3034.
(17) Reddy, G.; Chang, R.; Yethiraj, A. *J. Chem. Theory Comput.* **2006**, *2*, 630–636.
(18) Carrillo, J. Y.; Dobrynin, A. V. *Langmuir* **2007**, *23*, 2472–2482.
(19) Panwar, A. S.; Kumar, S. *J. Chem. Phys.* **2005**, *122*, −1-12.
(20) Raposo, M.; Mattoso, L. H. C.; Oliveira, O. N., Jr. *Thin Solid Films* **1998**, *327*, 739–742.
(21) Tekin, N.; Demirbas, Ö.; Alkan, M. *Microporous Mesoporous Mater.* **2005**, *85*, 340–350.
(22) Tekin, N.; Kadýncý, E.; Demirbaş, Ö.; Alkan, M.; Kara, A. *J. Colloid Interface Sci.* **2006**, *296*, 472–479.
(23) Tekin, N.; Dinçer, A.; Demirbaş, Ö.; Alkan, M. *J. Hazardous Mater.* **2006**, *134*, 211–219.
(24) Wallin, T.; Linse, P. *Langmuir* **1996**, *12*, 305–314.
(25) Wallin, T.; Linse, P. *J. Phys. Chem.* **1996**, *100*, 17873–17880.
(26) Wallin, T.; Linse, P. *J. Phys. Chem. B* **1997**, *101*, 5506–5513.
(27) Narambuena, C. F.; Beltramo, D. M.; Leiva, E. P. M. *Macromolecules* **2007**, *40*, 7336–7342.
(28) Naves, A. F.; Petri, D. F. S. *Colloids Surf. A* **2005**, *254*, 207–214.
(29) Reis, E. A. O.; Caraschi, J. C.; Carmona-Ribeiro, A. M.; Petri, D. F. S. *J. Phys. Chem. B* **2003**, *107*, 7993–7997.
(30) Narambuena, C. F.; Ausar, F. S.; Bianco, I. D.; Beltramo, D. M.; Leiva, E. P. M. *J. Agric. Food Chem.* **2005**, *53*, 459–463.
(31) *Understanding Molecular Simulation: From Algorithms to Applications*, 2nd ed.; Frenkel, D., Smit, B. Academic Press: San Diego, CA, 2001.
(32) Jarzynski, C. *Phys. Rev. Lett.* **1997**, *78*, 2690–2693.
(33) Jarzynski, C. *Phys. Rev. E* **1997**, *56*, 5018–5035.
(34) Liphardt, J.; Dumont, S.; Smith, S. B.; Tinoco, I., Jr.; Bustamante, C. *Science* **2002**, *296*, 1832–1835.
(35) Park, S.; Khalili-Araghi, F.; Tajkhorshid, E.; Schulten, K. *J. Chem. Phys.* **2003**, *119*, 3559–3566.
(36) Park, S.; Schulten, K. *J. Chem. Phys.* **2004**, *120*, 5946–5961.
(37) Gonzalez-Lebrero, M. C.; Estrin, D. A. *J. Chem. Theor. Comput.* **2007**, *3*, 1405–1411.
(38) Torrie, G. M.; Valleau, J. P. *J. Chem. Phys.* **1980**, *73*, 5807–5816.
(39) Boda, D.; Chan, K.; Henderson, D. J. *Chem. Phys.* **1998**, *109*, 7362–7371.
(40) *Monte Carlo and Molecular Dynamics Simulations in Polymer Science. Kurt Binder*; Oxford University Press: New York, 1995.
(41) *Intermolecular and Surface Forces*. Israelchvilli; J. N. Cornell University Press: Ithaca, NY, 1985.
(42) Lechner, W.; Dellago, C. *J. Stat. Mech.* **2007**, P04001.
(43) Kirkwood, J. G. *J. Chem. Phys.* **1935**, *3*, 300–313.
(44) Schmiedl, T.; Seifert, U. *J. Chem. Phys.* **2007**, *126*−1-12.
(45) Manning, G. S. *J. Chem. Phys.* **1969**, *51*, 924–933.
(46) Muthukumar, M. J. *Chem. Phys.* **2004**, *120*, 9343–9350.

MA800325E